Inducible Repression of Nuclear-Encoded Subunits of the Cytochrome b_6f Complex in Tobacco Reveals an Extraordinarily Long Lifetime of the Complex[1][W][OPEN]

Marta Hojka, Wolfram Thiele, Szilvia Z. Tóth[2], Wolfgang Lein[3], Ralph Bock, and Mark Aurel Schöttler*

Max-Planck-Institut für Molekulare Pflanzenphysiologie, Am Mühlenberg 1, D–14476 Potsdam-Golm, Germany

The biogenesis of the cytochrome b_6f complex in tobacco (*Nicotiana tabacum*) seems to be restricted to young leaves, suggesting a high lifetime of the complex. To directly determine its lifetime, we employed an ethanol-inducible RNA interference (RNAi) approach targeted against the essential nuclear-encoded Rieske protein (PetC) and the small M subunit (PetM), whose function in higher plants is unknown. Young expanding leaves of both *PetM* and *PetC* RNAi transformants bleached rapidly and developed necroses, while mature leaves, whose photosynthetic apparatus was fully assembled before RNAi induction, stayed green. In line with these phenotypes, cytochrome b_6f complex accumulation and linear electron transport capacity were strongly repressed in young leaves of both RNAi transformants, showing that the M subunit is as essential for cytochrome b_6f complex accumulation as the Rieske protein. In mature leaves, all photosynthetic parameters were indistinguishable from the wild type even after 14 d of induction. As RNAi repression of *PetM* and *PetC* was highly efficient in both young and mature leaves, these data indicate a lifetime of the cytochrome b_6f complex of at least 1 week. The switch-off of cytochrome b_6f complex biogenesis in mature leaves may represent part of the first dedicated step of the leaf senescence program.

The cytochrome b_6f complex (cyt-bf) functions as plastoquinol-plastocyanin oxidoreductase of photosynthetic electron transport in the thylakoid membrane of cyanobacteria and photosynthetic eukaryotes. It oxidizes plastoquinol previously reduced by the oxygen-evolving PSII and reduces plastocyanin, which then diffuses to PSI. The cyt-bf is the smallest multisubunit complex of the linear electron transport chain. Its active form is a dimer composed of eight different subunits with a total molecular mass of about 220 kD (Cramer et al., 2006; Baniulis et al., 2008). High-resolution structures of the cyt-bf have been obtained in the filamentous thermophilic cyanobacterium *Mastigocladus laminosus* (Kurisu et al., 2003; Hasan et al., 2013), in *Nostoc* sp. PCC 7120 (Baniulis et al., 2009), and in the unicellular eukaryotic alga *Chlamydomonas reinhardtii* (Stroebel et al., 2003).

Three subunits of the cyt-bf stably bind redox-active cofactors: plastoquinol oxidation occurs at the luminal plastoquinol-binding side, the p-side (Q_p). The first electron is transferred via the nuclear-encoded Rieske-2Fe2S-protein (PetC) and the plastome-encoded cytochrome f subunit (PetA) to plastocyanin. This first oxidation step generates a semiquinone radical, which acts as a strong reductant and transfers its second electron via the low-potential and high-potential hemes and possibly the heme c_n, which are all bound to cytochrome b_6 (PetB), to a stromal plastoquinone binding site as part of the Q-cycle. The plastome-encoded subunit IV, the product of the *petD* gene, does not stably bind any redox-active cofactors and is believed to mainly have a scaffold function but also forms part of the Q_P-site together with cytochrome b_6 (Cramer et al., 2006). All four large subunits are essential for the assembly of the cyt-bf in photosynthetic eukaryotes. In knockout mutants of the nuclear-encoded Rieske-2Fe2S-protein, the other subunits of the cyt-bf are still synthesized, but they cannot assemble into a complex (Bruce and Malkin, 1991; Maiwald et al., 2003). Therefore, they are instable and rapidly degraded so that no or only very low levels of most cyt-bf subunits are detectable (Bruce and Malkin, 1991; Maiwald et al., 2003). Notable species-dependent variations seem to exist for cytochrome f: In *Lemna perpusilla* (Bruce and Malkin, 1991) and tobacco (*Nicotiana tabacum*; Hager et al., 1999; Schwenkert et al., 2007), no cytochrome f accumulates in the absence of one of the other essential cyt-bf subunits, but both in *C. reinhardtii* and Arabidopsis (*Arabidopsis thaliana*), unassembled PetA can still be detected in the absence of the other

[1] This work was supported by the Deutsche Forschungsgemeinschaft (grant no. SFB429, project A12 to M.A.S. and R.B.) and the Alexander von Humboldt Foundation (research fellowship to S.Z.T.).

[2] Present address: Biological Research Centre of the Hungarian Academy of Sciences, Temesvári krt 62, H–6726, Szeged, Hungary.

[3] Present address: Technische Universität Berlin, Institut für Biotechnologie, Fachgebiet Bioanalytik, Seestrasse 13, D–1353 Berlin, Germany.

* Address correspondence to schoettler@mpimp-golm.mpg.de.

The author responsible for distribution of materials integral to the findings presented in this article in accordance with the policy described in the Instructions for Authors (www.plantphysiol.org) is: Mark Aurel Schöttler (schoettler@mpimp-golm.mpg.de).

[W] The online version of this article contains Web-only data.

[OPEN] Articles can be viewed online without a subscription.

www.plantphysiol.org/cgi/doi/10.1104/pp.114.243741

 © 2014 American Society of Plant Biologists. All Rights Reserved.

subunits of the cyt-bf (Kuras and Wollman, 1994; Maiwald et al., 2003).

In addition to the four large subunits, four small subunits with molecular masses of 3 to 4 kD are bound to each monomer of the cyt-bf (Baniulis et al., 2008). They form single transmembrane helices (hydrophobic sticks) and do not participate in any of the redox reactions of the complex. PetG and PetN are essential for cyt-bf assembly and stability, as evidenced by transplastomic knockout transformants in tobacco and *C. reinhardtii* not accumulating any cyt-bf (Berthold et al., 1995; Hager et al., 1999; Schwenkert et al., 2007). The other two small subunits, PetL and PetM, are located at the very periphery of the cyt-bf (Stroebel et al., 2003). The L subunit is nonessential, but its loss reduces the stability of the cyt-bf (Schöttler et al., 2007). The function of the last small subunit, the nuclear-encoded M subunit, has only been addressed in photosynthetic prokaryotes (Schneider et al., 2001). A PetM knockout mutant (Δ*petM*) of *Synechocystis* PCC 6803 accumulates wild-type levels of cyt-bf, while the accumulation of PSI and of phycobilisomes is reduced, suggesting a signaling function of PetM.

In higher plants, contents of the cyt-bf are highly responsive to environmental conditions and leaf development. The cyt-bf contents increase with actinic light intensity in higher plants, but the amplitudes of the changes are dependent on the species. For example, *Alocasia macrorrhiza* (Chow et al., 1988), barley (*Hordeum vulgare*; De la Torre and Burkey, 1990), and spinach (*Spinacia oleracea*; Chow and Hope, 1987) all retain relatively high cyt-bf contents in low light, and therefore the cyt-bf content increases less than 2-fold with light intensity. In pea (*Pisum sativum*; Evans, 1987) and tobacco (Petersen et al., 2011), more pronounced changes in cyt-bf contents with light intensity closely correlate with linear electron flux capacity. Calvin-Benson cycle activity and Rubisco content appear to be highly coregulated with the cyt-bf (Yamori et al., 2010). Also the ontogenetic decrease of leaf assimilation capacity in dicotyledons generally correlates well with changes in cyt-bf content. In bean (*Phaseolus vulgaris*), loss of the cyt-bf precedes the degradation of PSII, PSI, and chloroplast ATP synthase (Ben-David et al., 1983; Roberts et al., 1987). In tobacco, the decrease of assimilation capacity during leaf aging closely correlates with the ontogenetic loss of the cyt-bf but also of chloroplast ATP synthase and plastocyanin (Schöttler et al., 2004, 2007).

Plastoquinol reoxidation by the cyt-bf takes approximately 5 ms and therefore is almost one order of magnitude slower than the other reactions of linear electron flux (Haehnel, 1984; Hasan and Cramer, 2012). The maximum turnover number determined in isolated cyt-bf complexes is in the range of 250 to 300 electrons per complex per second (Pierre et al., 1995). In addition to its low enzymatic turnover number, the cyt-bf is usually present in, or at maximum, stoichiometric amounts relative to both photosystems (Whitmarsh and Ort, 1984; Chow and Anderson, 1987; Evans, 1987, 1988; Chow et al., 1988; De la Torre and Burkey, 1990; Anderson et al., 1997; Kirchhoff et al., 2002; Schöttler et al., 2004). Thus, plastoquinol reoxidation is the bottleneck of linear electron flux and should play a predominant role in photosynthetic flux control (Anderson, 1992; Schöttler and Tóth, 2014). It is noteworthy that in investigations published before 1997, cyt-bf contents may have been overestimated by 30%, because the difference extinction coefficient of cytochrome f has been substantially revised since then (Metzger et al., 1997), making a limiting function of the cyt-bf even more likely. A predominant role of the cyt-bf in photosynthetic flux control was ultimately confirmed by the specific inhibition of cyt-bf activity (Kirchhoff et al., 2000) and by an antisense approach against the Rieske protein (Price et al., 1995, 1998; Anderson et al., 1997; Yamori et al., 2011).

It is completely unknown how cyt-bf contents are adjusted to changes in environmental conditions and metabolic demand. In theory, the ratio of complex biogenesis to complex lifetime (i.e. protein complex turnover and degradation) could be altered. Cyt-bf biogenesis is dependent on the coordinated expression of its nuclear and chloroplast-encoded subunits. In *C. reinhardtii*, this is achieved by a complex mechanism of translational autoregulation in the chloroplast (Choquet et al., 2001), while transcript abundances at least in the plastid are not limiting (Eberhard et al., 2002). The translational regulation of cyt-bf biogenesis itself is dependent on nuclear-encoded factors involved in mRNA stability and translation initiation (Boulouis et al., 2011). Whether similar mechanisms operate in higher plants is unknown. The specific pathways required for heme synthesis and attachment to the apoproteins also could restrict cyt-bf biogenesis (Kuras et al., 2007; Lyska et al., 2007; Lezhneva et al., 2008; Gabilly et al., 2011). Moreover, for PSI accumulation, a limiting function of auxiliary proteins involved in its assembly has been demonstrated (Schöttler et al., 2011). Likewise, a limiting function of the recently identified DEFECTIVE IN THE ACCUMULATION OF THE CYTOCHROME B_6F COMPLEX protein, also named CONSERVED IN THE PLANTAE AND DIATOMS38 (Heinnickel et al., 2013), which is involved in PetD insertion into the complex (Xiao et al., 2012), cannot be excluded.

To our knowledge, the lifetime of the cyt-bf has not been determined in higher plants. Of all photosynthetic complexes, only the lifetime and turnover of PSII has been studied in detail (Aro et al., 2005; Rokka et al., 2005). In *C. reinhardtii*, cyt-bf contents declined slowly after inhibition of chloroplast translation by chloramphenicol, with a halftime of at least 1 d (Gong et al., 2001). However, due to the use of the translational inhibitor, it cannot be excluded that reactive oxygen species generated during PSII photoinhibition reduced the stability of the cyt-bf. We therefore decided to determine the lifetime of the cyt-bf in higher plants via the specific repression of de novo complex biogenesis. To this end, we used an inducible RNA interference (RNAi) approach against the essential nuclear-encoded Rieske protein and the M subunit, whose function has not been elucidated in plants. Our inducible RNAi approach provides clear evidence that, different from the situation in photosynthetic

prokaryotes, the M subunit is an essential component of the cyt-bf. Our data also show that cyt-bf biogenesis is restricted to young leaves, indicating that the lifetime of the complex is longer than 1 week.

RESULTS

Generation of Ethanol-Inducible *PetM* and *PetC* RNAi Plants

Tobacco 'Petit Havana' was transformed with ethanol-inducible RNAi constructs directed against the nuclear-encoded cyt-bf subunits PetC and PetM. As two highly homologous PetC isoforms exist in tobacco, which differ only in four amino acids and 15 nucleotides within the coding region, respectively (Madueño et al., 1992), we targeted both isoforms with our RNAi construct. The construct covered 211 nucleotides spanning positions 145 to 355 of the coding region of both isoforms. As the tobacco nuclear genome is not fully sequenced yet, searches of this unique fragment of *PetC* against all known tobacco ESTs (in the National Centre for Biotechnology Information and The Institute of Genomic Research) and against the Arabidopsis genome (in National Centre for Biotechnology Information and The Institute of Genomic Research) were performed to exclude off-target effects of our construct. These searches did not reveal any homologous sequences with more than 18-bp length; therefore, off-target silencing effects of the RNAi construct are unlikely to occur. Furthermore, this sequence is part of the 645-bp-long sequence used to generate the well-characterized tobacco Rieske-2Fe2S antisense plants (Price et al., 1995, 1998; Anderson et al., 1997; Yamori et al., 2011).

In the case of the inducible *PetM* RNAi construct, the situation was more difficult, as only an EST, but no full-length sequence information is available for tobacco. Therefore, we aligned this EST with *PetM* sequences from other Solanaceous species. Homologies were found to several open reading frames, which upon closer inspection turned out to be nonannotated versions of *PetM* from different species. No homologous sequence stretches of 21 bp or longer were found, making it unlikely that nonspecific silencing effects of the RNAi construct can occur.

For both RNAi constructs, we generated 50 independent transgenic lines by *Agrobacterium tumefaciens*-mediated transformation of tobacco leaf discs. For further analyses, transformed lines showing strong photosynthetic phenotypes after RNAi induction by ethanol treatment were selected. In the following, data from two exemplary lines are shown for each construct (lines nos. 48 and 50 for the *PetM* RNAi plants and lines nos. 2 and 27 for the *PetC* RNAi plants).

Inducible RNAi Repression of Both *PetC* and *PetM* Results in Visible Phenotypes Only in Young and Newly Forming Leaves

In the noninduced state, the transformants did not display a growth phenotype (as shown for one representative strong line of the *PetC* and *PetM* transformants in Supplemental Fig. S1A), indicating that the inducible RNAi constructs display no significant background activity. By contrast, after RNAi induction via ethanol evaporation, clear phenotypes developed. After 7 d of continuous induction, growth of the *PetM* and *PetC* RNAi plants was indistinguishable from the wild type, but those leaves of the transformants, which were still expanding during the induction, were partly bleached (Supplemental Fig. S1B). This phenotype is more visible in Figure 1, A to C, where detached leaves from the wild type and the induced RNAi transformants are shown. In young leaves, the phenotype was much more pronounced toward the leaf base, which represents the growing zone of the leaf, than at the tip of the leaf, where the photosynthetic apparatus was already established at the beginning of the induction. Near the leaf base, necrotic areas also became visible. However, in spite of this drastic phenotype of the newly formed leaves, even after 14 d of induction, no growth retardation of the transformants was observable (Supplemental Fig. S1C). Also, the onset of flowering was not significantly delayed in the RNAi lines.

To determine if the absence of a visible phenotype in the fully expanded leaves could be explained by a lower RNAi efficiency in mature than in young leaves, expression of the target genes was determined by northern blotting. As a control, expression of *PetC* in the *PetM* RNAi plants was also determined (Fig. 1D), and in the *PetC* RNAi plants, expression of *PetM* was assessed (Fig. 1E). Additionally, in both *PetM* and *PetC* RNAi plants, mRNA accumulation of *PsaD* encoding a stromal ridge subunit of PSI was determined. Finally, the accumulation of the chloroplast-encoded *petA* mRNA (encoding cytochrome f) was assessed. *petA* is the last gene in a tetracistronic operon also comprising *psaI* (encoding a small subunit of PSI), *ycf4* (encoding an auxiliary protein for PSI assembly), and the open reading frame *ycf10*. The primary operon transcript undergoes complex RNA processing, so that for *petA*, multiple RNA species are detectable (Krech et al., 2012).

Before RNAi induction, the accumulation of all mRNAs tested was indistinguishable between the wild type and the transformants. After 7 d of induction, the respective target gene was strongly repressed both in young, expanding leaves and in mature leaves, which were fully expanded prior to RNAi induction. This clearly shows that the absence of a visible phenotype in the mature leaves cannot be ascribed to a lower RNAi efficiency than in the young leaves displaying strong phenotypes. Interestingly, in mature leaves of the *PetM* RNAi plants, *PetC* expression was slightly higher than in the wild type. The same was observed for *PetM* in the *PetC* RNAi plants. Also, *PsaD* expression was slightly increased in mature leaves of both RNAi transformants. Northern-blot analysis using a *petA*-specific probe revealed no differences in operon processing or in transcript abundances. It is noteworthy that for mature leaves, after 7 d of RNA induction, more RNA had to be loaded to obtain detectable signals of the nuclear-encoded genes than for the uninduced leaves and for young leaves

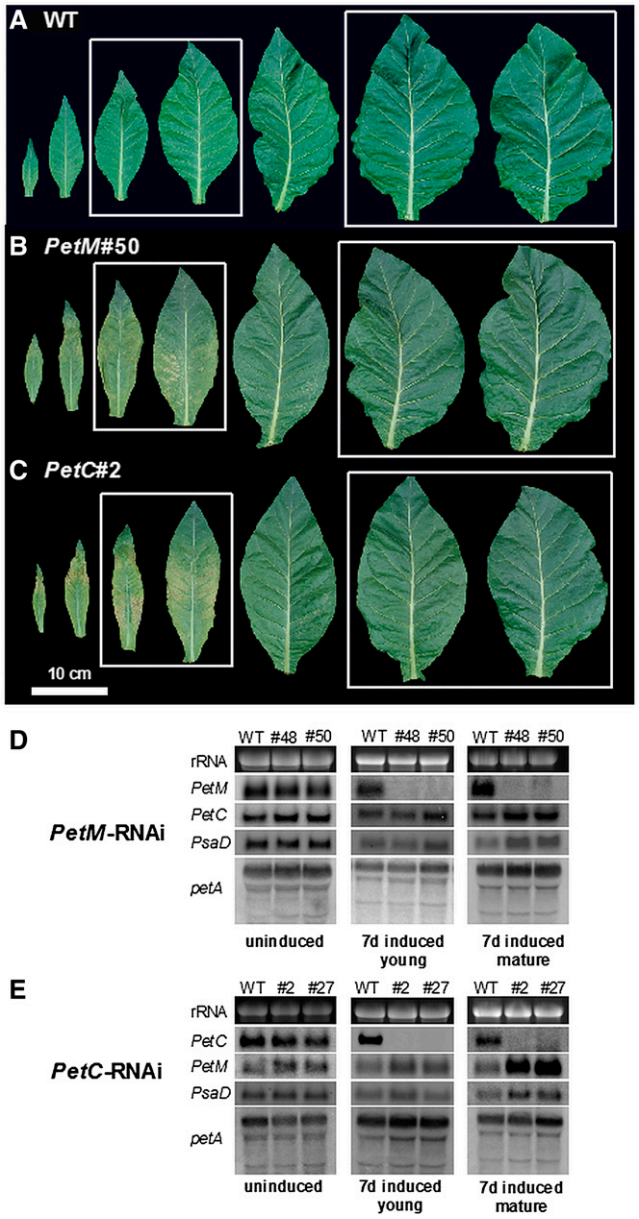

Figure 1. Phenotypes of detached leaves of wild-type (WT) tobacco (A), *PetM* RNAi plants (B), and *PetC* RNAi plants (C) harvested after 7 d of RNAi induction. The leaf pairs selected for detailed physiological analysis are boxed. Accumulation of the *PetM*, *PetC*, *PsaD*, and *petA* mRNAs in the *PetM* RNAi lines (D) and the *PetC* RNAi lines (E) was determined by northern-blot analyses. The ethidium bromide-stained 25S ribosomal RNA of the cytosolic 80S ribosomes is shown as a loading control.

after 7 d of induction. This strongly indicates a major reduction in mRNA abundance of photosynthetic genes with increasing leaf age (see below, Fig. 7).

Only Young Leaves Still Expanding at the Time of Induction Develop a Discernible Physiological Phenotype

We next determined a number of photosynthetic parameters in wild-type tobacco and the inducible RNAi plants. Prior to induction, we measured two fully expanded leaves and then remeasured these leaves after 7 and 14 d of induction. Additionally, after 7 d of induction, we measured young leaves that were still growing during the induction and therefore developed the partly bleached and necrotic phenotype. The selected leaves are boxed in Figure 1. The most strongly affected sectors of the young leaves showing massive bleaching and necrosis had to be excluded from all further analyses, because it was not possible to perform spectroscopic measurements on them. Therefore, the measurements shown in the following figures actually underestimate the severity of the phenotype in the young leaves after RNAi induction. Also, after 14 d of induction, the expanding leaves suffered from such massive damage that they had to be excluded from all analyses.

First, we determined leaf chlorophyll content (Supplemental Fig. S2A), leaf absorptance (Supplemental Fig. S2B), and the chlorophyll *a*/*b* ratio (Supplemental Fig. S2C). Because we excluded strongly damaged parts of the leaves from our analyses, the chlorophyll content per leaf area was not significantly different between the wild type and the transformants, even in young leaves after 7 d of induction. No significant leaf age-dependent changes in chlorophyll content and leaf absorptance could be observed. However, leaf absorptance tended to be lower in the young leaves of the transformants after 7 d of RNAi induction. The chlorophyll *a*/*b* ratio decreased from about 4.0 in young leaves to 3.5 in old leaves, indicating minor changes in the antenna sizes of the photosystems. No pronounced differences were observed between the wild type and the RNAi plants.

Also for the maximum photochemical efficiency of PSII in the dark-adapted state (F_v/F_m; Fig. 2A), no significant changes could be observed, even though there was a tendency toward lower F_v/F_m ratios in young leaves of the RNAi plants after 7 d of induction. A major effect was observed on the maximum capacity of linear electron transport (ETRII), as calculated from light response curves of the PSII operating efficiency (Fig. 2B). Maximum ETRII was corrected for the small differences in leaf absorptance (Supplemental Fig. S2B), and an equal distribution of absorbed excitation energy between the two photosystems was assumed (see also the paragraph on photosynthetic complex accumulation and antenna structure). While maximum linear electron flux was indistinguishable between wild-type and transformant leaves prior to induction and in mature leaves after 7 and 14 d of induction, it was strongly repressed in young leaves of the RNAi plants after 7 d of induction. This was expected in the case of the *PetC* RNAi plants, because the cyt-bf is the predominant site of photosynthetic flux control, and therefore any repression of its content should directly compromise linear electron flux capacity (Anderson, 1992; Price et al., 1995, 1998; Yamori et al., 2011). The severe repression of linear electron flux observed in *PetM* RNAi lines strongly suggests that the M subunit is also essential for the function and/or accumulation of the cyt-bf. The decrease of linear electron flux capacity from young to old leaves observed for both

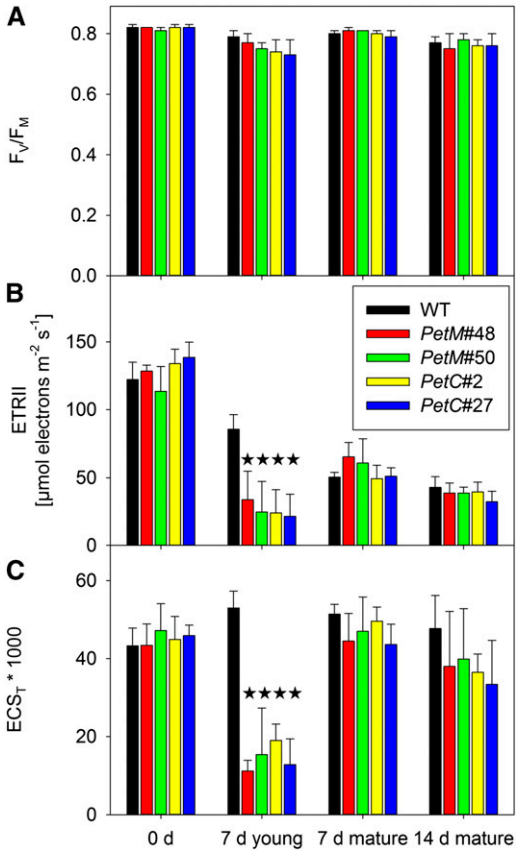

Figure 2. In vivo parameters of the photosynthetic apparatus before induction, after 7 d of induction in young, expanding leaves and in mature leaves (fully expanded prior to RNAi induction), and after 14 d of RNAi induction. A, F_v/F_m, an indicator of PSII efficiency. B, Maximum ETRII after correction for leaf absorptance. C, Maximum pmf across the thylakoid membrane, as determined from the ECS_T. Stars indicate significant differences relative to the wild type. WT, Wild type.

wild-type and RNAi plants is likely due to the ontogenetic down-regulation of cyt-bf contents in tobacco (Schöttler et al., 2004, 2007).

The proton motive force (pmf) across the thylakoid membrane was strongly decreased in young leaves of the RNAi lines after 7 d of induction (Fig. 2C). The pmf was determined from the total amplitude of the electrochromic shift signal (ECS_T) during a dark-interval relaxation kinetic (Baker et al., 2007). No significant differences could be observed in the noninduced state or in the mature leaves of the RNAi lines after 7 and 14 d of induction. The pmf remained high, even though in mature leaves, after 14 d of induction, linear electron flux was as low as in the young transformant leaves after 7 d of induction (Fig. 2, B and C). This can be explained by an adjustment of ATP synthase activity and/or content to the reduced linear electron flux capacity of old leaves (see below), so that proton influx into the lumen and proton efflux through the ATP synthase are rebalanced to allow maintenance of a high pmf, despite the strong down-regulation of linear electron flux (Schöttler et al., 2007; Rott et al., 2011).

To determine if the changes in linear electron flux and pmf formation in the young leaves also affect photoprotective mechanisms and the redox state of the PSII acceptor side, light response curves of the chlorophyll *a* fluorescence parameter nonphotochemical quenching (qN) and the redox state of the PSII acceptor side parameter (qL) were measured (Supplemental Fig. S3). Low values of qL indicated a strong reduction of the primary electron-accepting plastoquinone of PSII (Kramer et al., 2004; Baker et al., 2007). Prior to RNAi induction, the light response curves of qN and qL were indistinguishable between the wild type and the transformants (Supplemental Fig. S3A), in line with comparable electron transport rates and pmf formation. After 7 d of induction, nonphotochemical quenching was severely compromised in young leaves of the RNAi plants (Supplemental Fig. S3B). Also, the PSII acceptor side was much more rapidly reduced with increasing light intensity than in the wild type, which is consistent with the strong repression of linear electron flux (Supplemental Fig. S3B). For mature and old leaves of the transformants, after 7 (Supplemental Fig. S3C) and 14 d of induction (Supplemental Fig. S3D), no significant differences to the wild type could be observed. However, in line with the lower electron transport rates of mature and old leaves, qN induction and the reduction of the PSII acceptor side were shifted toward lower light intensities than in young leaves before induction.

Photosynthetic Complex Accumulation and Antenna Structure

Next, the major components of the photosynthetic apparatus were quantified in isolated thylakoids by spectroscopic techniques (Fig. 3) and immunoblots (Fig. 4). Again, the strongly bleached sectors of the leaves had to be excluded from all analyses, because no thylakoids could be isolated from these areas. The spectroscopic data were normalized on a leaf area basis. For PSII (Fig. 3A), no significant differences could be observed between the wild type and the transformants, independent of leaf age and developmental stage. Accumulation of the cyt-bf (Fig. 3B) was not significantly different between the wild type and the transformants prior to RNAi induction. In young leaves, after 7 d of induction, cyt-bf contents were strongly reduced relative to the wild type in both the *PetC* and *PetM* RNAi lines, well in agreement with the reduced linear electron flux capacity (Fig. 2B), the impaired pmf formation (Fig. 2C), and the impaired nonphotochemical quenching (Supplemental Fig. S3). In mature leaves, after neither 7 nor 14 days of induction, significant differences in cyt-bf contents could be detected between the wild type and the transformants, in accordance with their comparable rates of linear electron flux. With increasing leaf age, cyt-bf contents declined by about 50% per week, in line with previous observations in tobacco plants (Schöttler et al., 2004, 2007). Plastocyanin accumulation (Fig. 3C) did not differ significantly under any condition between the wild type and the RNAi lines. As for the cyt-bf,

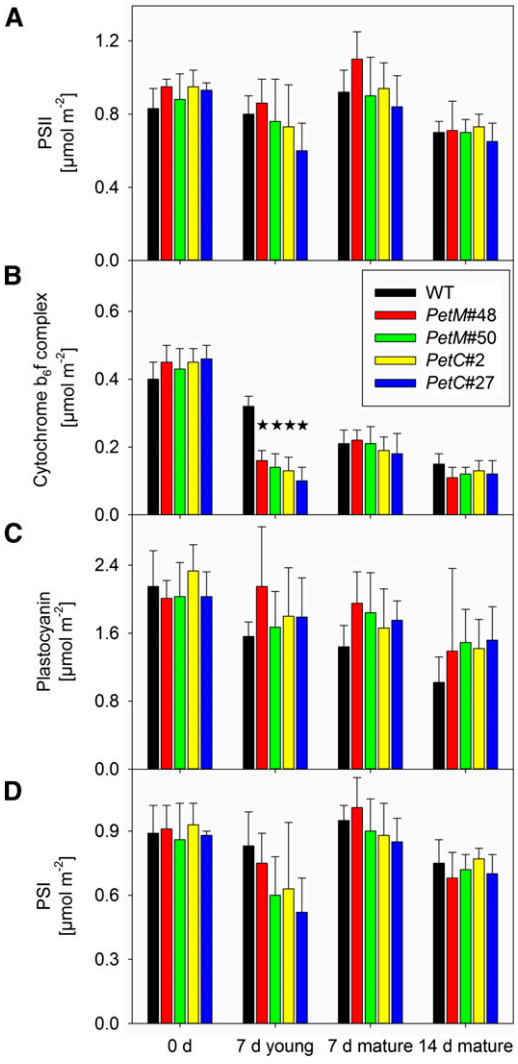

Figure 3. Photosynthetic complex accumulation per leaf area, as quantified via difference absorbance measurements in isolated thylakoids. A, PSII contents per leaf area, as determined from difference absorbance measurements of cytochrome b_{559}. B, The cyt-bf contents per leaf area, as determined by difference absorbance measurements of cytochromes f and b_6. C, Plastocyanin contents per leaf area, as determined from difference absorbance measurements in the far-red range of the spectrum. D, PSI contents per leaf area, as determined from difference absorbance measurements of the reaction center chlorophyll *a* dimer P_{700}. Stars indicate significant differences relative to the wild type. WT, Wild type.

an ontogenetic decline of plastocyanin contents from young to old leaves occurred but was somewhat less pronounced in the transformants. In the case of PSI (Fig. 3D), no significant differences between the wild type and the RNAi lines could be observed.

These spectroscopic quantifications were confirmed by immunoblot analyses of essential subunits of all photosynthetic complexes (Fig. 4). The immunoblots were performed with isolated thylakoids and loaded on an equal chlorophyll basis. For PSII, probed with antibodies against the PsbD reaction center subunit (D2 protein) and the PsbE subunit of cytochrome b_{559}, neither in the *PetM* RNAi plants (Fig. 4A) nor in the *PetC* RNAi plants (Fig. 4B), clear changes were observed. For the cyt-bf, the accumulation of cytochrome f (PetA), cytochrome b_6 (PetB), and the Rieske protein (PetC) was determined. The accumulation of all three tested subunits was indistinguishable between the wild type and the RNAi transformants before induction and in mature leaves after 7 and 14 d of induction. The ontogenetic repression of the cyt-bf from young to old leaves is clearly visible. In young leaves of the RNAi transformants, after 7 d of induction, the accumulation of all tested subunits including PetA was strongly repressed. These data show that the repressed linear electron flux in the *PetM* RNAi transformants cannot be explained by the accumulation of nonfunctional cyt-bf when the M subunit is absent but that PetM is as essential for the accumulation of the cyt-bf as the Rieske protein.

PSI accumulation was assessed by immunoblotting with antibodies against the reaction center subunits PsaA and PsaB. No changes between the wild type and the transformants or during leaf ontogenesis were observed. Finally, accumulation of the chloroplast ATP synthase was determined with an antibody against its catalytic β-subunit (AtpB). While no strong differences could be detected between the respective developmental states of the wild type and the transformants, an ontogenetic repression from young to old leaves was clearly visible. This parallel down-regulation of cyt-bf and ATP synthase balances proton efflux from the lumen through the ATP synthase to the diminished proton influx via photosynthetic electron transport and allows plants to maintain a high pmf, even in old leaves (Fig. 2C). The low pmf formation across the thylakoid membrane of young transformant leaves after 7 d of induction (Fig. 2C) correlates well with the specific loss of the cyt-bf, which is not paralleled by an adjustment of the ATP synthase (which remains at wild-type levels). The genetic knockdown of the cyt-bf uncouples the coregulation of cyt-bf and ATP synthase.

The conclusion that RNAi repression of the cyt-bf does not result in any major changes of the photosystems is further supported by 77-K chlorophyll *a* fluorescence emission spectra (Supplemental Fig. S4). Unaltered maximum emission wavelengths of PSII and its light harvesting complexes (LHCII) at 686 nm and of PSI-LHCI at 733 nm confirm that in all transformants, irrespective of the developmental state, the light-harvesting complexes are efficiently coupled to their reaction centers. Furthermore, similar ratios of the emission peaks of PSII-LHCII and PSI-LHCI under all developmental states demonstrate that the relative antenna cross sections of the photosystems do not change after RNAi induction and during leaf ontogenesis.

Both the M and the C Subunits Are Essential for the Assembly of the cyt-bf

To distinguish between a function of the M subunit already essential for complex assembly and a function

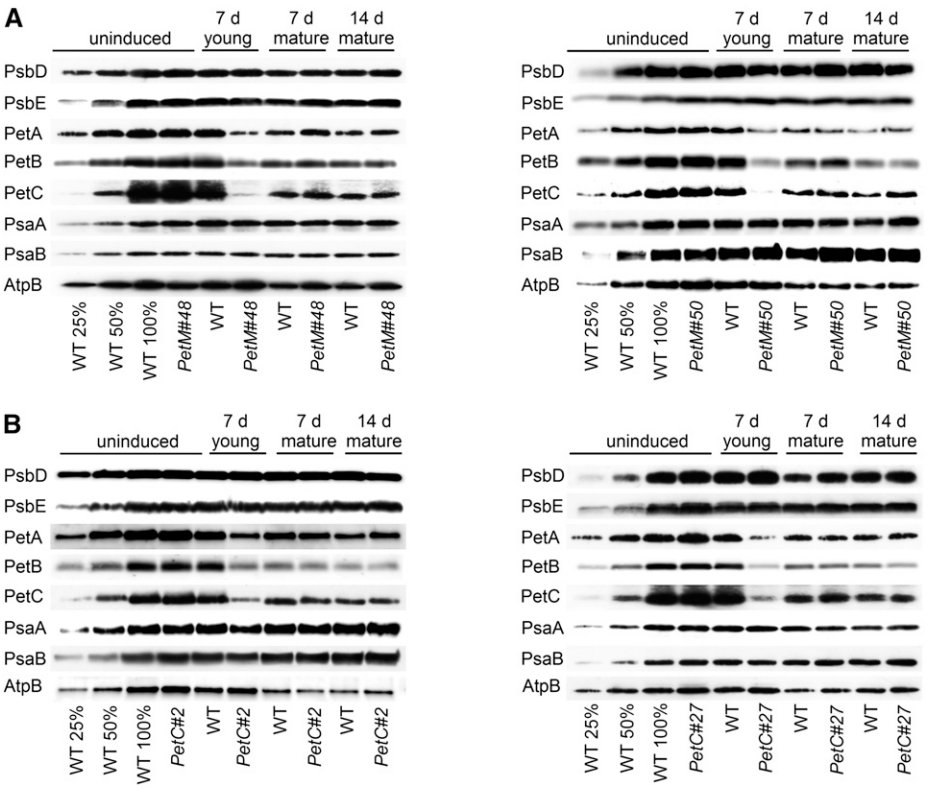

Figure 4. Immunoblots with antibodies against essential subunits of the photosynthetic protein complexes of wild-type (WT) tobacco and *PetC* and *PetM* transformants before and at different time points after RNAi induction. Isolated thylakoid membranes were used, and equal amounts of chlorophyll were loaded. For approximate quantification, wild-type samples harvested before RNAi induction were diluted to 25% and 50%, respectively. Accumulation of PSII was probed with antibodies against PsbD and PsbE. Accumulation of the cyt-bf was probed with antibodies against PetA, PetB, and PetC. Accumulation of PSI was probed with antibodies against the reaction center subunits PsaA and PsaB. ATP synthase accumulation was probed with an antibody against AtpB. A, Protein accumulation in wild-type tobacco and the two *PetM* RNAi transformants. B, Protein accumulation in wild-type tobacco and the two *PetC* RNAi transformants.

only related to complex stability, we determined cyt-bf contents in the first true leaves of young seedlings, which were just establishing their photosynthetic apparatus. In these leaves, cyt-bf biogenesis should proceed at its maximum rate. If the M subunit is only required for complex stability, but is not essential for complex assembly, higher amounts of the cyt-bf should be found in young leaves of the *PetM* RNAi lines than in leaves of the *PetC* RNAi mutants, because the Rieske protein has already been shown to be essential for complex assembly itself (Bruce and Malkin, 1991; Maiwald et al., 2003).

We grew seedlings at a low photon flux density of 20 μmol photons m^{-2} s^{-1} on agar-solidified synthetic medium with 2% (w/v) Suc and induced them directly after seed germination. All measurements were performed on the first true leaves, which were less than 1 cm long and strongly expanding at the time of the measurements. Light response curves of chlorophyll *a* fluorescence clearly demonstrated a massive impairment of photosynthesis in both the *PetC* and the *PetM* RNAi lines (Fig. 5A). No linear electron flux was measurable, and light response curves of qL revealed a complete reduction of the PSII acceptor side already at the lowest light intensity. To ultimately determine if the loss of the M subunit only impairs the stability of the cyt-bf in young leaves or if it is essential for the assembly of the complex, we isolated thylakoids from young leaves of 120 to 200 seedlings per line and quantified the abundances of the photosynthetic complexes by immunoblotting (Fig. 5B). At the low growth light intensity selected for the experiment, the accumulation of the two PSII subunits PsbD and PsbE, and the accumulation of chloroplast ATP synthase subunit AtpB were indistinguishable between the wild type and the RNAi lines. Accumulation of the PSI subunits PsaA and PsaB was slightly reduced in the RNAi lines. The accumulation of the cyt-bf subunits PetA, PetB, and PetC was strongly decreased in all RNAi lines. In the *PetC* RNAi lines, accumulation of the Rieske-2Fe2S-protein was decreased to less than 10% of wild-type amounts. In the two *PetM* RNAi lines, between 10% and 20% of wild-type amounts of the Rieske protein were still detectable. PetA contents dropped to less than 10% of wild-type levels in all RNAi lines. Accumulation of PetB varied between 10% and 20% of wild-type amounts. The comparable defects in cyt-bf protein accumulation in the *PetM* and *PetC* RNAi lines strongly suggest that both M and C subunits are essential for the assembly of the cyt-bf.

Light Stress Does Not Reinduce the Biogenesis of the cyt-bf in Mature Leaves

To assess if the biogenesis of the cyt-bf can be reinduced in mature leaves in response to needs created by environmental perturbations, we aimed at identifying photosynthetic parameters that are easily measurable in vivo and can be used as simple and reliable noninvasive indicators for the cyt-bf content. To this end,

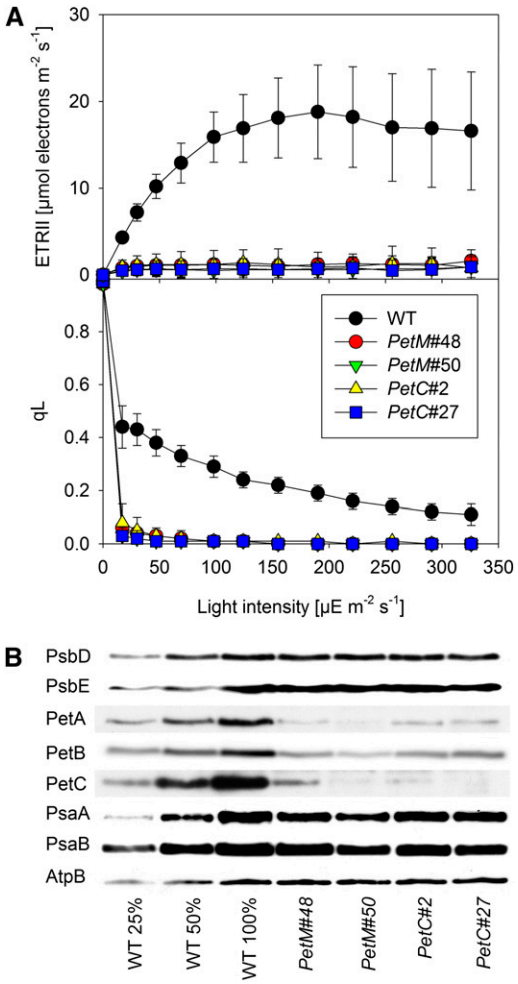

Figure 5. Photosynthetic parameters of the first true leaves of constitutively induced seedlings of *PetM* and *PetC* RNAi lines. A, Light response curves of linear electron flux and the chlorophyll *a* fluorescence parameter qL measured in the first true leaves of seedlings after germination under constitutively induced growth conditions. At least 10 independent replicates were measured for the wild type (WT) and the different RNAi lines. Error bars represent the SD. B, Immunoblots with antibodies against essential subunits of the photosynthetic protein complexes. Isolated thylakoid membranes were used for the blots, and equal amounts of chlorophyll were loaded. For approximate quantification, wild-type samples were diluted to 25% and 50%, respectively. The same antibodies as in Figure 4 were used.

we correlated the cyt-bf content (Fig. 3B) with several photosynthetic parameters, which can be measured in vivo. The best correlation was observed for the maximum ETRII, well in line with a predominant role of the cyt-bf in photosynthetic flux control (Fig. 6A). This predominant function of the cyt-bf in photosynthetic flux control in all measured plants and developmental states is also supported by the enzymatic turnover numbers of the cyt-bf, which can be obtained by dividing the maximum ETRII through the corresponding cyt-bf content. Under all conditions, turnover numbers between 200 and 300 electrons per cyt-bf per second were obtained, close to the maximum turnover numbers known for the cyt-bf (Pierre et al., 1995). Therefore, the maximum ETRII can be used as noninvasive measure to follow changes in cyt-bf content.

We tested if the biogenesis of the cyt-bf can be reinduced in mature leaves after transfer to high-light conditions to cope with increased oxidative stress and to adjust photosynthetic capacity to the increased light intensity. Therefore, we grew plants at 250 μmol photons m^{-2} s^{-1} actinic light intensity, which is slightly lower than the light intensity used for the previous experiments, and then exposed them to a 4-fold increase in light intensity by shifting them to 1000 μmol photons m^{-2} s^{-1}. Ethanol induction of the RNAi constructs began immediately after the high-light transfer. Photosynthetic parameters of young, newly developing leaves and of mature leaves were measured prior to the high-light transfer (day 0) and during the following 7 d. As controls, young and mature leaves of plants maintained at 250 μmol photons m^{-2} s^{-1} light intensity were also measured. Measurements were performed on the two *PetM* RNAi lines (nos. 48 and 50) and the two *PetC* RNAi lines (nos. 2 and 27) characterized before. Because we did not observe significant differences between the lines, average values for the two *PetM* and the two *PetC* RNAi lines are shown in Figure 6, B to E.

At 250 μmol photons m^{-2} s^{-1}, already after 3 d of induction, linear electron flux (Fig. 6B) declined significantly in young leaves. After 5 d of induction, linear electron flux was repressed to less than 20% of the wild-type capacity in both *PetM* and *PetC* RNAi lines. From day 5 to 7 of induction, only a minor further decline of linear electron flux occurred. Mature leaves displayed the typical leaf age-related decline of linear electron flux (Fig. 6C), but no significant differences between the wild type and the RNAi plants could be observed, even after 7 d of induction, in line with our previous observations (Fig. 2B). Also, at 1,000 μmol photons m^{-2} s^{-1}, young leaves of the RNAi lines displayed a significant decrease of linear electron flux capacity (Fig. 6D) already after 3 d of induction, and linear electron flux decreased further until 7 d of induction. The young wild-type leaves, however, did not differ from young leaves under standard growth conditions. Again, no difference in linear electron flux capacity (Fig. 6E) was observed between mature wild-type and mutant leaves.

After 7 d of induction, we quantified the photosynthetic complexes in mature leaves grown under a light intensity of 250 or 1,000 μmol photons m^{-2} s^{-1}. In line with the in vivo measurements of linear electron flux capacity, we could not observe any significant differences in cyt-bf content between the wild-type plants and the RNAi mutants under either growth condition (Table I). However, we observed clear differences between leaves grown under standard conditions and high-light conditions. At 1,000 μmol photons m^{-2} s^{-1}, the chlorophyll content per leaf area decreased by about 30% in the wild type and the RNAi plants. In line with a lower chlorophyll *a*/*b* ratio, the contents of both photosystems decreased by 25% to 40%, relative to the control plants. The cyt-bf content decreased at least by 25%. The decreased

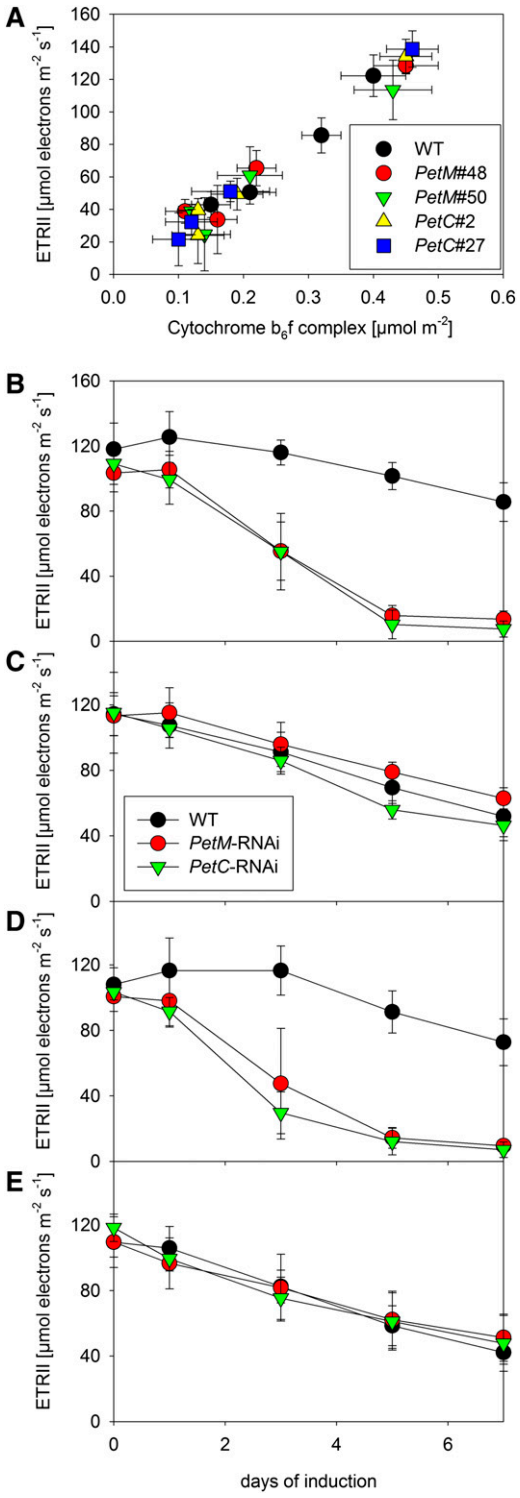

Figure 6. ETRII as an in vivo measure of cyt-bf content. A, Correlation between light-saturated linear electron transport capacity per leaf area with cyt-bf contents per leaf area. B to E, Changes in linear electron transport capacity in young, expanding (B and D) and mature leaves (C and E) of wild-type (WT) tobacco and RNAi plants under standard growth conditions (B and C; 250 μmol photons m^{-2} s^{-1}) and during 7 d of high-light stress (D and E; 1,000 μmol photons m^{-2} s^{-1}). Error bars represent the SD.

F_v/F_m value suggests that under high-light conditions, all plants suffered from moderate oxidative stress.

Decreased Transcript Abundances of Both Plastid- and Nuclear-Encoded Subunit of the cyt-bf Could Be Causal for the Ontogenetic Repression of cyt-bf Biogenesis

Finally, to determine if transcriptional regulation contributes to the ontogenetic decrease of cyt-bf content in mature leaves, we compared the mRNA abundances of chloroplast- and nuclear-encoded subunits of the cyt-bf between young and mature wild-type leaves (Fig. 7). Among the plastid-encoded genes, only the mRNA abundances of *petG* and *petN* were significantly decreased in mature leaves, while the transcript abundances of *petB* and *petD* were not reduced, in line with previous observations (Schöttler et al., 2007). The small decrease in mRNA accumulation of *petA* and *petL* in mature leaves was not significant. However, the abundance of the nuclear-encoded *PetC* and *PetM* mRNAs was clearly decreased. A similar result was also obtained for the expression of exemplarily investigated nuclear-encoded subunits of the two photosystems and the chloroplast ATP synthase: mRNA abundances of *PsaD*, *PsaF*, *PsbO*, *PsbY*, and *AtpC* were reduced in mature leaves (Fig. 7).

DISCUSSION

Lifetime of the cyt-bf in Higher Plants

Our current knowledge about lifetimes and protein turnover rates of photosynthetic complexes in higher plants is still very much limited. However, such knowledge is essential to understand how photosynthetic complex biogenesis and photosynthetic complex accumulation can be adjusted to changing environmental conditions and metabolic demands. The lifetime of PSII is by far the shortest of all complexes, especially under light stress conditions, when the D1 reaction center protein suffers from oxidative damage caused by singlet oxygen (Krieger-Liszkay, 2005). In the most extreme cases, D1 can be damaged at a rate as high as once per hour (He and Chow, 2003) and therefore has to be efficiently replaced by the PSII repair cycle (Aro et al., 2005). In contrast to the detailed investigations of the lifetime and the repair cycle of PSII, the lifetimes of all other photosynthetic complexes have not been directly assessed in higher plants. In the green alga *C. reinhardtii*, inhibition of chloroplast translation by chloramphenicol resulted in rapid loss of PSII, while the decay of the cyt-bf was slower, with a halftime well above 21 h (Gong et al., 2001). In this situation, the accumulation of damaged PSII might decrease the stability of the photosynthetic apparatus in general, due to increased production of reactive oxygen species. Therefore, inhibition of chloroplast translation is not a suitable approach to determine the lifetimes of photosynthetic complexes. Furthermore, the unicellular alga *C. reinhardtii* can hardly be compared to higher plants, because the cultured algal cells are constantly

Table I. *Chlorophyll a/b ratio, chlorophyll content per leaf area, F_v/F_m, and contents of PSII, the cyt-bf, plastocyanin, and PSI of mature leaves of wild-type plants and the inducible PetM and PetC RNAi mutants grown either under standard growth conditions (250 μmol photons m^{-2} s^{-1}) or under high-light conditions (1,000 μmol photons m^{-2} s^{-1})*

All parameters were determined after 7 d of RNAi induction. Average values and SDs for a minimum of five individual plants are given. For no parameter, a significant difference between the wild type and the RNAi-lines was observed.

Parameter	Wild Type (250 μmol)	*PetM* RNAi (250 μmol)	*PetC* RNAi (250 μmol)	Wild Type (1,000 μmol)	*PetM* RNAi (1,000 μmol)	*PetC* RNAi (1,000 μmol)
Chlorophyll *a/b*	3.56 ± 0.16	3.52 ± 0.08	3.49 ± 0.12	3.27 ± 0.22	3.42 ± 0.33	3.38 ± 0.30
Chlorophyll (mg m^{-2})	546.6 ± 33.5	524.7 ± 30.0	475.7 ± 54.8	372.3 ± 24.0	366.1 ± 49.5	410.9 ± 38.9
F_v/F_m	0.79 ± 0.02	0.80 ± 0.01	0.79 ± 0.02	0.71 ± 0.03	0.72 ± 0.04	0.71 ± 0.04
PSII (μmol m^{-2})	1.24 ± 0.20	1.21 ± 0.13	1.10 ± 0.14	0.81 ± 0.10	0.90 ± 0.14	0.89 ± 0.13
cyt-bf (μmol m^{-2})	0.32 ± 0.03	0.29 ± 0.07	0.27 ± 0.02	0.20 ± 0.03	0.22 ± 0.03	0.21 ± 0.04
Plastocyanin (μmol m^{-2})	1.69 ± 0.33	1.98 ± 0.25	1.51 ± 0.28	1.30 ± 0.32	1.52 ± 0.37	1.73 ± 0.25
PSI (μmol m^{-2})	1.21 ± 0.10	1.22 ± 0.09	1.07 ± 0.13	0.72 ± 0.08	0.70 ± 0.08	0.82 ± 0.11

growing and dividing, a situation which is, at best, comparable to the situation in very young expanding leaves of higher plants. In fully expanded leaves, protein synthesis rates are much lower, as the photosynthetic apparatus only needs to be maintained and little de novo biogenesis may occur (Fleischmann et al., 2011).

In higher plants, loss of the small plastome-encoded L subunit destabilizes the cyt-bf but does not alter cyt-bf accumulation in young expanding leaves. Only in mature leaves does a strongly accelerated leaf age-dependent loss of the cyt-bf and, consequently, of linear electron flux and assimilation occur (Schöttler et al., 2007). Presumably, young leaves compensate for the reduced stability of the cyt-bf in the Δ*petL* mutant by an increased complex assembly, while in older leaves, the reduced stability of the cyt-bf cannot be compensated by de novo synthesis anymore. This suggests a strong ontogenetic down-regulation of cyt-bf biogenesis once leaves are fully expanded. If one would assume that biogenesis is completely switched off, the slow decline in cyt-bf contents with increasing leaf age in wild-type tobacco (Schöttler et al., 2007) could directly reflect its lifetime.

To directly assess the lifetime of the cyt-bf, we have pursued an approach based on the inducible RNAi repression of its two nuclear-encoded subunits. While PetC is essential for cyt-bf assembly (Bruce and Malkin, 1991; Maiwald et al., 2003), the role of the small M subunit is still unknown in plants. A tightly regulated inducible system should not result in any repression of the target gene in the noninduced state. Neither for the *PetC* nor for the *PetM* RNAi lines was any difference observed in the levels of mRNA accumulation of the target gene (Fig. 1, D and E). Also, plant growth (Supplemental Fig. S1A) and all physiological parameters analyzed did not reveal significant differences between the wild type and the noninduced RNAi mutants (Figs. 2–4; Supplemental Figs. S2–S4).

A pronounced phenotype could only be observed in young leaves of the RNAi mutants, which were still expanding at the time of induction, while no discernible phenotype could be observed in mature leaves, whose photosynthetic apparatus was fully established prior to RNAi induction. These differences cannot be attributed to different RNAi efficiencies in young versus mature leaves (Fig. 1, D and E). In young, newly developing leaves, cyt-bf accumulation is severely compromised (Fig. 3), and the effects on all photosynthetic parameters are similar to those previously reported for constitutive *PetC* antisense mutants (Price et al., 1995, 1998; Anderson et al., 1997; Yamori et al., 2011). Linear electron flux and pmf formation are strongly impaired (Fig. 2). As a consequence, photoprotective nonphotochemical quenching is compromised, and the PSII acceptor side is strongly reduced (Supplemental Fig. S3). This overreduction, in combination with the reduced capacity of nonphotochemical quenching, likely results in increased production of reactive oxygen species. In those parts of the leaves where reactive oxygen species production exceeds a critical threshold level, cell death pathways are initiated (Danon et al., 2006; Kim et al., 2008), thus explaining the necrotic spots visible on young leaves after RNAi induction (Fig. 1, B and C). By contrast, leaves that had fully expanded prior to the RNAi

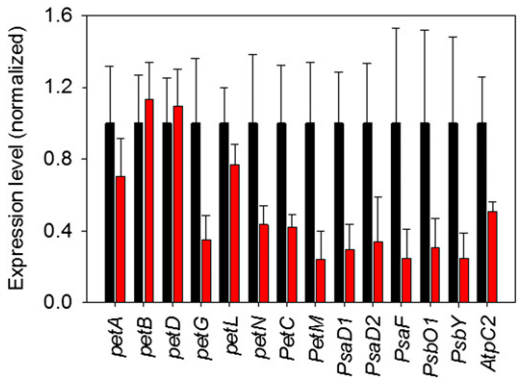

Figure 7. qRT-PCR analyses to quantify mRNA abundances of all plastid-encoded and the two nuclear-encoded subunits of the cyt-bf in young (black bars) and mature leaves (red bars) of wild-type tobacco. The mRNA abundance of nuclear-encoded genes for subunits of PSI (*PsaD* and *PsaF*) and PSII (*PsbO1* and *PsbY*) and the ATP synthase (*AtpC2*) was also determined. Gene expression in young leaves was normalized to one. Error bars represent the SD.

induction did not show any significant difference to wild-type plants. This can only be explained with a high lifetime of the cyt-bf and a restriction of its biogenesis to young, expanding leaves. Consequently, RNAi repression of the nuclear-encoded subunits of the cyt-bf does not affect the photosynthetic apparatus once it is fully established (as in mature leaves), simply because electron transport runs with preexisting complexes and no de novo synthesis of PetC and PetM is required.

While our data indicate an extraordinarily high lifetime of the nuclear-encoded C and M subunits of the cyt-bf, we cannot formally exclude the possibility that some of the plastid-encoded subunits of the complex have shorter lifetimes. If this were the case, these less stable plastid-encoded subunit(s) would have to be replaced with high efficiency to prevent proteolytic degradation of the partially disassembled complex. However, no evidence for such a cyt-bf repair cycle exists, and there is no specific subunit of the cyt-bf that is particularly prone to photodamage. This is because its reactions occur at much more moderate redox potentials than oxygen evolution in PSII. Also, the lifetime of the singlet excited state of the structural chlorophyll *a* molecule in the cyt-bf is very short, so that production of singlet oxygen should be effectively prevented (Dashdorj et al., 2005).

Ontogenetic Repression of cyt-bf Biogenesis in Mature Leaves

Our data strongly indicate that in tobacco, cyt-bf biogenesis is restricted to young leaves. Therefore, the slow decay in cyt-bf contents during leaf aging (Schöttler et al., 2007) is likely to reflect the minimum lifetime of the complex. This may have implications for our understanding of the ontogenetic program of the plant in that ceased synthesis of the cyt-bf may represent one of the first dedicated steps during leaf aging, which occurs weeks before any symptoms of leaf senescence, such as reduced leaf pigmentation, become visible.

Whether the cyt-bf is actively degraded in mature leaves to rebalance linear electron flux to the ontogenetic down-regulation of the Calvin-Benson cycle remains to be elucidated. The accelerated loss of the cyt-bf, together with both photosystems, in mature leaves during the growth under high-light conditions (Table I) could be due to active degradation of all complexes. It also seems possible that the loss is triggered by damage to the complexes due to mild oxidative stress, as suggested by the decreased F_v/F_m value (Table I). In *C. reinhardtii*, both the ATP-dependent caseinolytic protease (Clp) and the filamenting temperature-sensitive mutant H (FtsH) protease have been implied in rapid degradation of the cyt-bf under sulfur- and nitrogen-limited growth conditions (Majeran et al., 2000; Malnoë et al., 2014; Wei et al., 2014), but in higher plants, no comparable conditions that would result in a rapid degradation of the cyt-bf are known.

Likewise, the molecular mechanism underlying the ontogenetic repression of cyt-bf biogenesis in mature leaves is still unknown and warrants further analysis. Decreased transcript accumulation of some plastid-encoded and all nucleus-encoded subunits of the cyt-bf in mature leaves suggests an involvement of transcriptional regulation or regulation of RNA stability (Fig. 7). A purely transcriptional regulation might be difficult to achieve, especially for those plastid-encoded cyt-bf subunits, which are parts of polycistronic transcripts. *petB* and *petD* are the last two genes of a large operon also comprising the three PSII genes *psbB*, *psbT*, and *psbH*, while *petA* is the final gene of a large operon also encoding *psaI*, the PSI assembly factor *ycf4*, and *ycf10*. In particular, the *psbB-psbT-psbH-petB-petD* operon undergoes complex posttranscriptional processing, but its mRNA accumulation does not change during leaf ontogenesis in tobacco (Schöttler et al., 2007). The unaltered expression level of the operon might be due to the fact that in addition to D1 and D2, PsbH is the PSII subunit most prone to oxidative damage, and therefore, it also has a rapid turnover during the PSII repair cycle (Rokka et al., 2005). Therefore, regulation of RNA abundance is unlikely to be solely responsible for the ontogenetic loss of the cyt-bf. In the chloroplast, gene expression is mainly controlled at the level of translation (Eberhard et al., 2002), so that a reduced translation of the plastid-encoded subunits could mediate the ontogenetic decline in cyt-bf. Also, nuclear-encoded factors involved in cofactor synthesis and their insertion into the apoproteins of the complex could be down-regulated in mature leaves and, in this way, contribute to the ontogenetic demise of the cyt-bf. Dedicated pathways for heme insertion into PetA and PetB exist, and in addition, specific chaperones are required for cyt-bf assembly (Lennartz et al., 2006; Kuras et al., 2007; Lyska et al., 2007; Lezhneva et al., 2008; Gabilly et al., 2011; Xiao et al., 2012; Heinnickel et al., 2013). However, a down-regulation at the late stage of cofactor synthesis or cyt-bf assembly would be a rather inefficient and wasteful process and, therefore, seems less likely.

The high lifetime and slow turnover of the cyt-bf may not be an unusual feature of bioenergetic protein complexes in higher plants. Because the Ycf3-interacting protein1 (Y3IP1) and Ycf4, two auxiliary proteins required for PSI accumulation, only accumulate in young leaves, Krech et al. (2012) suggested that PSI biogenesis might also be restricted to young tobacco leaves. Based on the comparison of protein biosynthesis rates to total protein abundances in Arabidopsis, Piques et al. (2009) calculated that the lifetimes of different enzymes of primary metabolism vary between a few hours and up to 3 weeks, with the majority of the Calvin-Benson cycle enzymes ranging between 2 d and more than 1 week. Finally, a ^{15}N-labeling study performed in Arabidopsis revealed remarkably high lifetimes for the bioenergetic complexes of the respiratory electron transport chain (Nelson et al., 2013): among all major mitochondrial protein complexes, complex III showed the largest variation in the protein degradation rates of its different subunits, but the majority of its subunits had a degradation rate of less than 0.1 per day. This indicates similar lifetimes of the mitochondrial cytochrome bc_1 complex and its chloroplast homolog, the cyt-bf.

Molecular Function of the M Subunit

The phenotypes of the *PetM* RNAi plants are indistinguishable from those of the *PetC* RNAi plants, indicating that the M subunit is essential for cyt-bf accumulation. More precisely, because even in very young leaves of seedlings, which just establish their photosynthetic apparatus and assemble the cyt-bf at a high rate, accumulation of cyt-bf subunits is as strongly affected in the *PetM* RNAi lines as in the *PetC* RNAi lines, the M subunit seems to be essential already for cyt-bf assembly (Fig. 5B). This starkly differs from a tobacco transformant affected in the nonessential L subunit, which is only required for complex stability but not for the assembly of the cyt-bf (Schöttler et al., 2007). The proposed function of the M subunit in cyt-bf assembly is consistent with the three-dimensional structure of the cyt-bf: PetM seems to strongly interact with the structural β-carotene bound to each cyt-bf monomer (Stroebel et al., 2003; Cramer et al., 2006). It is also located in close proximity to the other two essential small subunits, PetG (Schwenkert et al., 2007) and PetN (Hager et al., 1999). Interestingly, in *Synechocystis* PCC 6803, the M subunit is nonessential and is thought to exert a regulatory function by controlling the accumulation of other photosynthetic and respiratory complexes (Schneider et al., 2001). This major difference in PetM function between cyanobacteria and higher plants cannot be easily explained, as the structures of the cyanobacterial cyt-bf obtained in *M. laminosus* (Kurisu et al., 2003) and the cyt-bf of photosynthetic eukaryotes (Stroebel et al., 2003) are very similar. However, the M subunit shows by far the lowest level of sequence identity of all cyt-bf subunits between *M. laminosus* and *Synechocystis* sp. PCC 6803 (Baniulis et al., 2009). Thus, it seems possible that the M subunit in *Synechocystis* sp. PCC 6803 has adopted a somewhat different function.

Our data demonstrate that inducible RNAi repression of essential nuclear-encoded subunits of the photosynthetic complexes represents a feasible approach to obtain information on the lifetimes of these complexes. Therefore, a systematic study of the lifetimes of all components of the photosynthetic apparatus should now be possible. For example, the lifetimes of the chloroplast ATP synthase and PSI should be easily determinable, because essential subunits of both complexes are encoded in the nuclear genome. In the case of the ATP synthase, both the γ-subunit (AtpC) and the δ-subunit (AtpD) would be suitable candidates, while in the case of PSI, the two nuclear-encoded proteins constituting the stromal ridge, PsaD and PsaE, appear to be the best candidates. Precise knowledge of photosynthetic complex lifetimes will strongly improve our understanding of how photosynthetic complex accumulation can be adjusted to ever-changing environmental conditions and metabolic demands.

MATERIALS AND METHODS

Plant Material and Growth Conditions

Tobacco (*Nicotiana tabacum*) transformants were raised from seeds germinated in petri dishes containing Murashige and Skoog medium supplemented with 2% (w/v) Suc (Murashige and Skoog, 1962) and 250 μg mL^{-1} of kanamycin for selection. For constitutive induction of RNAi constructs, immediately after germination, seedlings were transferred to boxes containing Murashige and Skoog medium supplemented with 2% (w/v) Suc but without antibiotics. For measurements with plants grown under autotrophic conditions, seedlings were transferred 14 d after germination to a soil:vermiculite mixture (2:1) and grown in a controlled environment chamber at 120 μmol photons m^{-2} s^{-1} light intensity (16-h day, 22°C, and 75% relative humidity). Night temperature and relative humidity were reduced to 18°C and 70%, respectively. Five weeks after germination, the plants were transferred to a growth chamber (Conviron). The actinic light intensity on the level of the youngest leaves was approximately 300 μmol photons m^{-2} s^{-1}. Day length and humidity were unaltered (i.e. 16-h day and 75% humidity). After 14 d of growth under these conditions, the RNAi construct was induced by continuous evaporation of ethanol in the growth chamber.

Generation of the Inducible RNAi Constructs

For ethanol-inducible RNAi repression, the plasmid system designed by Chen et al. (2003) was used. Briefly, this plasmid system contains an *alcR* gene, an ethanol-responsive transcription factor from *Aspergillus nidulans*. The *alcR* gene is expressed under the control of the strong constitutive *Cauliflower mosaic virus* 35S promoter and the nopaline synthase (*nos*) terminator of *Agrobacterium tumefaciens*. Inserts containing the selected unique fragment of the gene of interest (see "Results") in sense and antisense orientation, separated by an intron, were cloned behind a modified *alcA* promoter, whose activity is dependent on the ethanol-induced binding of the AlcR transcription factor. Transformation of the *PetC* RNAi and *PetM* RNAi constructs into tobacco 'Petit Havana' was done by *A. tumefaciens*-mediated gene transfer using bacterial strain C58C1:pGV2260 (Rosahl et al., 1987).

RNA Gel-Blot Analyses

RNA was extracted from tobacco leaves using the peqGold Trifast reagent (PeqLab). Samples equivalent to 10 to 30 μg of RNA were separated in 1% (w/v) formaldehyde-containing agarose gels and blotted onto Hybond-XL nylon membranes. A *PetC*-specific probe was generated by PCR amplification from complementary DNA (cDNA) with the primers PPetCfw (5′-GCTACAAGTATTCCAGCAGATG-3′) and PPetCrev (5′-GCCATTCAGATGCAATGACATC-3′). The *PetM*-specific probe was generated by PCR amplification from cDNA with the primers PPetMfw (5′-AGGTACAAGGATGTCTTCCCAG-3′) and PPetMrev (5′-TTGAAGACAGAGCTCCACCTTTG-3′). The *PsaD*-specific probe was generated by PCR amplification from cDNA with the primers PPsaDfw (5′-TTGAGATGCCAACTGGTGGTG-3′) and PPsaDrev (5′-GCTCTTGTTCTTACCAATGGATC-3′). The *petA*-specific probe was generated by PCR amplification from genomic DNA with the primers PpetAfw (5′-GCACAGCAGGGTTATGAAAATCC-3′) and PpetADrev (5′-CCTTCCCCTGTTCCCGCCTACG-3′). For hybridization, α[^{32}P]dCTP-labeled probes were generated by random priming (Multiprime DNA Labeling Kit, GE Healthcare) following the protocol of the manufacturer. Hybridizations were carried out overnight at 65°C in hybridization buffer (1% [w/v] bovine serum albumin, 1 mM EDTA, 7% [w/v] SDS, and 0.5 M $NaHPO_4$, pH 7.2). Signals were quantified using a Typhoon Trio+ variable mode imager (GE Healthcare) and the Image Quant 5.2 software.

qRT-PCR

Primers for the real-time reverse transcription-PCR analysis were designed as described by Albus et al. (2012). The melting temperature was set to 60°C, the amplicon length was set between 50 and 180 bp, and the guanine-cytosin content of the amplicon varied between 35% and 65% (Supplemental Table S1). To remove DNA from the samples, the isolated RNA was treated with the TURBO DNA-Free Kit (Life Technologies). To confirm the absence of DNA contaminations, an aliquot of the RNA sample was used as template in a PCR using primers targeting the tobacco *petG* gene. After confirmation of the absence of DNA contaminations, RNA integrity was checked on a 1% (w/v) denaturing agarose gel. One microgram of RNA was then used for cDNA synthesis with Super Script III reverse transcriptase (Life Technologies). Real-time quantitative reverse transcription (qRT)-PCR analysis was performed using a StepOnePlus Real-Time PCR System (Applied Biosystems) using Absolute SYBR Green ROX Mix (Thermo Scientific). To ensure correct normalization of the investigated genes, we tested the expression level of 10 potential reference genes described in Arabidopsis (*Arabidopsis thaliana*; Czechowski et al., 2005) and tobacco (Schmidt and Delaney, 2010). The three reference genes showing the most stable gene expression during leaf ontogenesis were a ubiquitin-conjugating enzyme E2 (homologous to At2g02760), a SAND family protein (homologous to At2g28390),

and a clathrin adaptor protein (homologous to At5g46630). Five biological replicates were measured with three technical replicates each.

Chlorophyll *a* Fluorescence

Chlorophyll *a* fluorescence emission at 77 K was determined on freshly isolated thylakoids equivalent to 10 μg of chlorophyll mL^{-1} using a F-6500 fluorometer (Jasco). The sample was excited at a 430-nm wavelength (10-nm bandwidth). Emission spectra between 655 and 800 nm were recorded with a bandwidth of 1 nm.

Chlorophyll *a* fluorescence of intact leaves was measured at 22°C using a Dual-PAM-100 instrument (Heinz Walz). F_v/F_m and light-response curves of ETRII and qN (Krause and Weis, 1991) as well as of qL (Kramer et al., 2004) were measured on intact leaves after at least 30 min of dark adaptation. When young leaves were measured after 7 d of induction, the necrotic leaf areas were avoided. To calculate linear electron transport rates for each actinic light intensity, the PSII operating efficiency was multiplied with the corresponding photosynthetically active photon flux density, assuming equal distribution of excitation energy between the two photosystems. The linear electron transport rates were corrected for the leaf absorptance measured with an integrating sphere (ISV-469, Jasco) attached to a spectrophotometer (V-550, Jasco). Transmittance and reflectance spectra of leaves were recorded between 400 and 700 nm wavelength, and leaf absorptance was calculated as 100% minus transmittance of light through the leaf minus reflectance on the leaf surface. The average value of the absorptance spectrum between 400 and 700 nm wavelength was used for the calculation of linear electron flux, assuming an equal distribution of absorbed light between both photosystems. Light response curves of photosynthesis in seedlings grown under mixotrophic conditions were measured using the MAXI version of the Imaging-PAM (Heinz Walz).

pmf Measurements

The electrochromic absorption shift (ECS) was used as an in vivo probe of the pmf across the thylakoid membrane (Baker et al., 2007). The difference transmission signal was measured using a KLAS-100 LED-Array Spectrophotometer (Heinz Walz), allowing the simultaneous measurement of light-induced difference absorption signals at eight pairs of wavelengths in the visible range of the spectrum between 505 and 570 nm, as described by Rott et al. (2011). In this wavelength range, in addition to the ECS, difference transmission signals originating from the zeaxanthin-violaxanthin interconversion and from PsbS protonation, the C550 pheophytin signal, and the difference transmission signals of cytochromes b_6, f, and b_{559} also occur. The ECS was deconvoluted from these signals as described by Klughammer et al. (1990). The deconvoluted transmission signals ($\Delta I/I$) were then normalized to the chlorophyll content of the measured leaf section. The ECS_T was used as a measure for the light-induced pmf across the thylakoid membrane. Leaves were illuminated for 10 min prior to each measurement to allow photosynthesis to reach steady state. ECS_T was determined after illuminating the leaves with saturating light (2,100 μmol photons m^{-2} s^{-1}), which then was interrupted by a short interval of darkness (15 s), and the dark-interval relaxation of the ECS was measured. Signal amplitudes were normalized to the leaf chlorophyll content, which was determined in 80% (v/v) acetone according to Porra et al. (1989).

Thylakoid Membrane Isolation and Quantification of Photosynthetic Complexes

Thylakoid membranes were isolated from green sectors of the leaves, according to Schöttler et al. (2004). The contents of PSII and the cyt-bf were determined from difference absorption signals of cytochromes b_{559} (PSII) and f and b_6. Thylakoids equivalent to 50 μg of chlorophyll mL^{-1} were destacked in a low-salt medium to improve the optical properties of the probe (Kirchhoff et al., 2002). All cytochromes were oxidized by the addition of 1 mM potassium ferricyanide (+III) and subsequently reduced by addition of 10 mM sodium ascorbate and dithionite, resulting in the reduction of cytochrome f and the high-potential form of cytochrome b_{559} (ascorbate-ferricyanide difference spectrum) and cytochrome b_6 and the low-potential form of cytochrome b_{559}, respectively. At each redox potential, absorption spectra were measured between 575 and 540 nm wavelength with a V-550 spectrophotometer (Jasco) equipped with a head-on photomultiplier. The spectral bandwidth was 1 nm, and the scanning speed was 100 nm min^{-1}. Difference absorption spectra were deconvoluted using reference spectra and difference extinction coefficients as in Kirchhoff et al. (2002). PSII contents were calculated from the sum of the high- and low-potential difference absorption signals of cytochrome b_{559} (Lamkemeyer et al., 2006).

The content of redox-active PSI was determined from light-induced difference absorption changes of P_{700}, the PSI reaction center chlorophyll *a* special pair dimer. Isolated thylakoids equivalent to 50 μg of chlorophyll mL^{-1} were solubilized with 0.2% (w/v) β-dodecylmaltoside in the presence of 100 μM paraquat as electron acceptor and of 10 mM sodium ascorbate as electron donor. P_{700} was oxidized by the application of a saturating light pulse (2,000 μmol photons m^{-2} s^{-1} red light, 200-ms duration). Measurements were done using the plastocyanin-P_{700} version of the Dual-PAM instrument (Heinz Walz).

Plastocyanin contents relative to P_{700} were determined by in vivo difference absorption spectroscopy in the far-red range of the spectrum and then recalculated based on the absolute P_{700} quantification in isolated thylakoids (see above). Light-induced absorption changes at 800 to 870 nm wavelength (where the contribution of P_{700} is predominant) and at 870 to 950 nm wavelength (where signals predominantly arise from plastocyanin) were measured on preilluminated leaves with a fully activated Calvin-Benson cycle to avoid an acceptor side limitation of PSI (Schöttler et al., 2007). To determine the maximum difference absorption signals of plastocyanin and PSI, preilluminated leaves were transferred into darkness for 10 s to fully reduce both components, and this was followed by 8 s of illumination with far-red light (715-nm wavelength) to selectively excite PSI. Then, a saturating pulse of red light was applied (635-nm wavelength, 5,000 μmol photons m^{-2} s^{-1}, and 200-ms duration) to completely oxidize plastocyanin and PSI and reduce the PSII side of the electron transport chain. At the end of the actinic light pulse, all light sources were switched off, and plastocyanin and PSI were fully reduced again.

Protein Gel Electrophoresis and Western Blotting

Thylakoid proteins separated by SDS-PAGE (Perfect Blue twin gel system, Peqlab) were transferred to a polyvinylidene difluoride membrane (Hybond P) using a tank blotting system (Perfect Blue Web M, PeqLab). Specific polyclonal antibodies (produced in rabbits) against PsbD, PsbE, PetA, PetB, PetC, PsaA, PsaB, and AtpB were purchased from AgriSera AB. As secondary antibody, an anti-rabbit IgG peroxidase conjugate was used (Sigma-Aldrich). Immunochemical detection was carried out with the ECL Prime System (GE Healthcare), according to the instructions of the manufacturer.

Statistics

Four independent RNAi induction experiments were carried out. In vivo data represent averages of eight different leaves. As leaves were pooled for thylakoid isolations (Fig. 1, A–C), four independent replicates were obtained for the in vitro quantifications of photosynthetic complexes. Significance analyses were performed using an ANOVA with a pairwise multiple comparison procedure (Holm-Sidak method) in SigmaPlot. Error bars represent the SD.

Supplemental Data

The following materials are available in the online version of this article.

Supplemental Figure S1. Growth phenotypes of wild-type tobacco, a representative line of the *PetC* RNAi plants, and a representative line of the *PetM* RNAi plants before induction, after 7 d, and after 14 d of continuous RNAi induction by ethanol evaporation in the growth chamber.

Supplemental Figure S2. In vivo parameters of the photosynthetic apparatus before induction, after 7 d of induction in young expanding leaves and in mature leaves (fully expanded prior to RNAi induction), and after 14 d of RNAi induction.

Supplemental Figure S3. Light response curves of the chlorophyll *a* fluorescence qN and qL in wild-type tobacco and *PetM* and *PetC* RNAi lines before induction, in young, expanding and mature, fully expanded leaves after 7 d of induction, and in mature, fully expanded leaves after 14 d of induction.

Supplemental Figure S4. Chlorophyll *a* fluorescence emission spectra at 77 K measured in isolated thylakoids of wild-type tobacco and two lines of *PetM* and *PetC* transformants.

Supplemental Table S1. Overview of primers used for qRT-PCR analyses shown in Figure 7.

ACKNOWLEDGMENTS

We thank Dr. Daniel Karcher for help with vector construction, Brigitte Buchwald for plant transformation, and Britta Hausmann, Helga Kulka, and Saskia Rheinhardt for plant cultivation.

Received May 26, 2014; accepted June 24, 2014; published June 24, 2014.

LITERATURE CITED

Albus CA, Salinas A, Czarnecki O, Kahlau S, Rothbart M, Thiele W, Lein W, Bock R, Grimm B, Schöttler MA (2012) LCAA, a novel factor required for magnesium protoporphyrin monomethylester cycle accumulation and feedback control of aminolevulenic acid biosynthesis in tobacco. Plant Physiol **160:** 1923–1939

Anderson JM (1992) Cytochrome b 6 f complex: dynamic molecular organization, function and acclimation. Photosynth Res **34:** 341–357

Anderson JM, Price GD, Chow WS, Hope AB, Badger MR (1997) Reduced levels of cytochrome bf complex in transgenic tobacco leads to marked photochemical reduction of the plastoquinone pool, without significant change in acclimation to irradiance. Photosynth Res **53:** 215–227

Aro EM, Suorsa M, Rokka A, Allahverdiyeva Y, Paakkarinen V, Saleem A, Battchikova N, Rintamäki E (2005) Dynamics of photosystem II: a proteomic approach to thylakoid protein complexes. J Exp Bot **56:** 347–356

Baker NR, Harbinson J, Kramer DM (2007) Determining the limitations and regulation of photosynthetic energy transduction in leaves. Plant Cell Environ **30:** 1107–1125

Baniulis D, Yamashita E, Whitelegge JP, Zatsman AI, Hendrich MP, Hasan SS, Ryan CM, Cramer WA (2009) Structure-function, stability, and chemical modification of the cyanobacterial cytochrome b_6f complex from *Nostoc* sp. PCC 7120. J Biol Chem **284:** 9861–9869

Baniulis D, Yamashita E, Zhang H, Hasan SS, Cramer WA (2008) Structure-function of the cytochrome b_6f complex. Photochem Photobiol **84:** 1349–1358

Ben-David H, Nelson N, Gepstein S (1983) Differential changes in the amount of protein complexes in the chloroplast membrane during senescence of oat and bean leaves. Plant Physiol **73:** 507–510

Berthold DA, Schmidt CL, Malkin R (1995) The deletion of petG in *Chlamydomonas reinhardtii* disrupts the cytochrome bf complex. J Biol Chem **270:** 29293–29298

Boulouis A, Raynaud C, Bujaldon S, Aznar A, Wollman FA, Choquet Y (2011) The nucleus-encoded *trans*-acting factor MCA1 plays a critical role in the regulation of cytochrome *f* synthesis in *Chlamydomonas* chloroplasts. Plant Cell **23:** 333–349

Bruce BD, Malkin R (1991) Biosynthesis of the chloroplast cytochrome b_6f complex: studies in a photosynthetic mutant of *Lemna*. Plant Cell **3:** 203–212

Chen S, Hofius D, Sonnewald U, Börnke F (2003) Temporal and spatial control of gene silencing in transgenic plants by inducible expression of double-stranded RNA. Plant J **36:** 731–740

Choquet Y, Wostrikoff K, Rimbault B, Zito F, Girard-Bascou J, Drapier D, Wollman FA (2001) Assembly-controlled regulation of chloroplast gene translation. Biochem Soc Trans **29:** 421–426

Chow WS, Anderson JM (1987) Photosynthetic responses of *Pisum sativum* to an increase in irradiance during growth II. Thylakoid membrane components. Aust J Plant Physiol **14:** 9–19

Chow WS, Hope AB (1987) The stoichiometries of supramolecular complexes in thylakoid membranes from spinach chloroplasts. Aust J Plant Physiol **14:** 21–28

Chow WS, Qian L, Goodchild DJ, Anderson JM (1988) Photosynthetic acclimation of *Alocasia macrorrhiza* (L.) G. Don to growth irradiance: structure, function, and composition of chloroplasts. Aust J Plant Physiol **15:** 107–122

Cramer WA, Zhang H, Yan J, Kurisu G, Smith JL (2006) Transmembrane traffic in the cytochrome b_6f complex. Annu Rev Biochem **75:** 769–790

Czechowski T, Stitt M, Altmann T, Udvardi MK, Scheible WR (2005) Genome-wide identification and testing of superior reference genes for transcript normalization in Arabidopsis. Plant Physiol **139:** 5–17

Danon A, Coll NS, Apel K (2006) Cryptochrome-1-dependent execution of programmed cell death induced by singlet oxygen in *Arabidopsis thaliana*. Proc Natl Acad Sci USA **103:** 17036–17041

Dashdorj N, Zhang H, Kim H, Yan J, Cramer WA, Savikhin S (2005) The single chlorophyll *a* molecule in the cytochrome b_6f complex: unusual optical properties protect the complex against singlet oxygen. Biophys J **88:** 4178–4187

De la Torre WR, Burkey KO (1990) Acclimation of barley to changes in light intensity: photosynthetic electron transport activity and components. Photosynth Res **24:** 127–136

Eberhard S, Drapier D, Wollman FA (2002) Searching limiting steps in the expression of chloroplast-encoded proteins: relations between gene copy number, transcription, transcript abundance and translation rate in the chloroplast of *Chlamydomonas reinhardtii*. Plant J **31:** 149–160

Evans JR (1987) The relationship between electron transport components and photosynthetic capacity in pea leaves grown at different irradiances. Aust J Plant Physiol **14:** 157–170

Evans JR (1988) Acclimation by the thylakoid membranes to growth irradiance and the partitioning of nitrogen between soluble and thylakoid proteins. Aust J Plant Physiol **15:** 93–106

Fleischmann TT, Scharff LB, Alkatib S, Hasdorf S, Schöttler MA, Bock R (2011) Nonessential plastid-encoded ribosomal proteins in tobacco: a developmental role for plastid translation and implications for reductive genome evolution. Plant Cell **23:** 3137–3155

Gabilly ST, Kropat J, Karamoko M, Page MD, Nakamoto SS, Merchant SS, Hamel PP (2011) A novel component of the disulfide-reducing pathway required for cytochrome c assembly in plastids. Genetics **187:** 793–802

Gong XS, Chung S, Fernández-Velasco JG (2001) Electron transfer and stability of the cytochrome b_6f complex in a small domain deletion mutant of cytochrome f. J Biol Chem **276:** 24365–24371

Haehnel W (1984) Photosynthetic electron transport in higher plants. Annu Rev Plant Physiol **35:** 659–693

Hager M, Biehler K, Illerhaus J, Ruf S, Bock R (1999) Targeted inactivation of the smallest plastid genome-encoded open reading frame reveals a novel and essential subunit of the cytochrome b_6f complex. EMBO J **18:** 5834–5842

Hasan SS, Cramer WA (2012) On rate limitations of electron transfer in the photosynthetic cytochrome b_6f complex. Phys Chem Chem Phys **14:** 13853–13860

Hasan SS, Stofleth JT, Yamashita E, Cramer WA (2013) Lipid-induced conformational changes within the cytochrome b_6f complex of oxygenic photosynthesis. Biochemistry **52:** 2649–2654

He J, Chow WS (2003) The rate coefficient of repair of photosystem II after photoinactivation. Physiol Plant **118:** 297–304

Heinnickel ML, Alric J, Wittkopp T, Yang W, Catalanotti C, Dent R, Niyogi KK, Wollman FA, Grossman AR (2013) Novel thylakoid membrane GreenCut protein CPLD38 impacts accumulation of the cytochrome b_6f complex and associated regulatory processes. J Biol Chem **288:** 7024–7036

Kim C, Meskauskiene R, Apel K, Laloi C (2008) No single way to understand singlet oxygen signalling in plants. EMBO Rep **9:** 435–439

Kirchhoff H, Horstmann S, Weis E (2000) Control of the photosynthetic electron transport by PQ diffusion microdomains in thylakoids of higher plants. Biochim Biophys Acta **1459:** 148–168

Kirchhoff H, Mukherjee U, Galla HJ (2002) Molecular architecture of the thylakoid membrane: lipid diffusion space for plastoquinone. Biochemistry **41:** 4872–4882

Klughammer C, Kolbowski J, Schreiber U (1990) LED array spectrophotometer for measurement of time resolved difference spectra in the 530-600 nm wavelength region. Photosynth Res **25:** 317–327

Kramer DM, Johnson G, Kiirats O, Edwards GE (2004) New fluorescence parameters for the determination of Q_a redox state and excitation energy fluxes. Photosynth Res **79:** 209–218

Krause GH, Weis E (1991) Chlorophyll-*a* fluorescence and photosynthesis: the basics. Annu Rev Plant Physiol Plant Mol Biol **42:** 313–349

Krech K, Ruf S, Masduki FF, Thiele W, Bednarczyk D, Albus CA, Tiller N, Hasse C, Schöttler MA, Bock R (2012) The plastid genome-encoded Ycf4 protein functions as a nonessential assembly factor for photosystem I in higher plants. Plant Physiol **159:** 579–591

Krieger-Liszkay A (2005) Singlet oxygen production in photosynthesis. J Exp Bot **56:** 337–346

Kuras R, Saint-Marcoux D, Wollman FA, de Vitry C (2007) A specific c-type cytochrome maturation system is required for oxygenic photosynthesis. Proc Natl Acad Sci USA **104:** 9906–9910

Kuras R, Wollman FA (1994) The assembly of cytochrome b_6f complexes: an approach using genetic transformation of the green alga *Chlamydomonas reinhardtii*. EMBO J **13:** 1019–1027

Kurisu G, Zhang H, Smith JL, Cramer WA (2003) Structure of the cytochrome b_6f complex of oxygenic photosynthesis: tuning the cavity. Science **302:** 1009–1014

Lamkemeyer P, Laxa M, Collin V, Li W, Finkemeier I, Schöttler MA, Holtkamp V, Tognetti VB, Issakidis-Bourguet E, Kandlbinder A, et al (2006) Peroxiredoxin Q of *Arabidopsis thaliana* is attached to the thylakoids and functions in context of photosynthesis. Plant J **45:** 968–981

Lennartz K, Bossmann S, Westhoff P, Bechtold N, Meierhoff K (2006) HCF153, a novel nuclear-encoded factor necessary during a post-translational step in biogenesis of the cytochrome bf complex. Plant J **45:** 101–112

Lezhneva L, Kuras R, Ephritikhine G, de Vitry C (2008) A novel pathway of cytochrome c biogenesis is involved in the assembly of the cytochrome b_6f complex in Arabidopsis chloroplasts. J Biol Chem **283:** 24608–24616

Lyska D, Paradies S, Meierhoff K, Westhoff P (2007) HCF208, a homolog of *Chlamydomonas* CCB2, is required for accumulation of native cytochrome b6 in *Arabidopsis thaliana*. Plant Cell Physiol **48:** 1737–1746

Madueño F, Napier JA, Cejudo FJ, Gray JC (1992) Import and processing of the precursor of the Rieske FeS protein of tobacco chloroplasts. Plant Mol Biol **20:** 289–299

Maiwald D, Dietzmann A, Jahns P, Pesaresi P, Joliot P, Joliot A, Levin JZ, Salamini F, Leister D (2003) Knock-out of the genes coding for the Rieske protein and the ATP synthase delta subunit of Arabidopsis: effects on photosynthesis, thylakoid protein composition, and nuclear chloroplast gene expression. Plant Physiol **133:** 191–202

Majeran W, Wollman FA, Vallon O (2000) Evidence for a role of ClpP in the degradation of the chloroplast cytochrome b_6f complex. Plant Cell **12:** 137–150

Malnoë A, Wang F, Girard-Bascou J, Wollman FA, de Vitry C (2014) Thylakoid FtsH protease contributes to photosystem II and cytochrome b_6f remodeling in *Chlamydomonas reinhardtii* under stress conditions. Plant Cell **26:** 373–390

Metzger SU, Cramer WA, Whitmarsh J (1997) Critical analysis of the extinction coefficient of chloroplast cytochrome f. Biochim Biophys Acta **1319:** 233–241

Murashige T, Skoog F (1962) A revised medium for rapid growth and bioassays with tobacco tissue culture. Physiol Plant **15:** 473–497

Nelson CJ, Li L, Jacoby RP, Millar AH (2013) Degradation rate of mitochondrial proteins in *Arabidopsis thaliana* cells. J Proteome Res **12:** 3449–3459

Petersen K, Schöttler MA, Karcher D, Thiele W, Bock R (2011) Elimination of a group II intron from a plastid gene causes a mutant phenotype. Nucleic Acids Res **39:** 5181–5192

Pierre Y, Breyton C, Kramer D, Popot JL (1995) Purification and characterization of the cytochrome b_6f complex from *Chlamydomonas reinhardtii*. J Biol Chem **270:** 29342–29349

Piques M, Schulze WX, Höhne M, Usadel B, Gibon Y, Rohwer J, Stitt M (2009) Ribosome and transcript copy numbers, polysome occupancy and enzyme dynamics in Arabidopsis. Mol Syst Biol **5:** 314

Porra RJ, Thompson WA, Kriedermann PE (1989) Determination of accurate extinction coefficient and simultaneous equations for essaying chlorophylls *a* and *b* extracted with four different solvents: verification of the concentration of chlorophyll standards by atomic absorption spectroscopy. Biochim Biophys Acta **975:** 384–394

Price GD, von Caemmerer S, Evans JR, Siebke K, Anderson JM, Badger MR (1998) Photosynthesis is strongly reduced by antisense suppression of chloroplastic cytochrome bf complex in transgenic tobacco. Aust J Plant Physiol **25:** 445–452

Price GD, Yu JW, von Caemmerer S, Evans JR, Chow WS, Anderson JM, Hurry V, Badger MR (1995) Chloroplast cytochrome b_6f and ATP synthase complexes in tobacco: transformation with antisense RNA against nuclear-encoded transcripts for the Rieske FeS and ATPδ polypeptides. Aust J Plant Physiol **22:** 285–297

Roberts DR, Thompson JE, Dumbroff EB, Gepstein S, Mattoo AK (1987) Differential changes in the synthesis and steady-state levels of thylakoid proteins during bean leaf senescence. Plant Mol Biol **9:** 343–353

Rokka A, Suorsa M, Saleem A, Battchikova N, Aro EM (2005) Synthesis and assembly of thylakoid protein complexes: multiple assembly steps of photosystem II. Biochem J **388:** 159–168

Rosahl S, Schell J, Willmitzer L (1987) Expression of a tuber-specific storage protein in transgenic tobacco plants: demonstration of an esterase activity. EMBO J **6:** 1155–1159

Rott M, Martins NF, Thiele W, Lein W, Bock R, Kramer DM, Schöttler MA (2011) ATP synthase repression in tobacco restricts photosynthetic electron transport, CO_2 assimilation, and plant growth by overacidification of the thylakoid lumen. Plant Cell **23:** 304–321

Schmidt GW, Delaney SK (2010) Stable internal reference genes for normalization of real-time RT-PCR in tobacco (*Nicotiana tabacum*) during development and abiotic stress. Mol Genet Genomics **283:** 233–241

Schneider D, Berry S, Rich P, Seidler A, Rögner M (2001) A regulatory role of the PetM subunit in a cyanobacterial cytochrome b_6f complex. J Biol Chem **276:** 16780–16785

Schöttler MA, Albus CA, Bock R (2011) Photosystem I: its biogenesis and function in higher plants. J Plant Physiol **168:** 1452–1461

Schöttler MA, Flügel C, Thiele W, Bock R, Bock R (2007) Knockout of the plastid-encoded PetL subunit results in reduced stability and accelerated leaf age-dependent loss of the cytochrome b_6f complex. J Biol Chem **282:** 976–985

Schöttler MA, Kirchhoff H, Weis E (2004) The role of plastocyanin in the adjustment of the photosynthetic electron transport to the carbon metabolism in tobacco. Plant Physiol **136:** 4265–4274

Schöttler MA, Tóth SZ (2014) Photosynthetic complex stoichiometry dynamics in higher plants: environmental acclimation and photosynthetic flux control. Front Plant Sci **5:** 188

Schwenkert S, Legen J, Takami T, Shikanai T, Herrmann RG, Meurer J (2007) Role of the low-molecular-weight subunits PetL, PetG, and PetN in assembly, stability, and dimerization of the cytochrome b_6f complex in tobacco. Plant Physiol **144:** 1924–1935

Stroebel D, Choquet Y, Popot JL, Picot D (2003) An atypical haem in the cytochrome b_6f complex. Nature **426:** 413–418

Wei L, Derrien B, Gautier A, Houille-Vernes L, Boulouis A, Saint-Marcoux D, Malnoë A, Rappaport F, de Vitry C, Vallon O, et al (2014) Nitric oxide-triggered remodeling of chloroplast bioenergetics and thylakoid proteins upon nitrogen starvation in *Chlamydomonas reinhardtii*. Plant Cell **26:** 353–372

Whitmarsh J, Ort DR (1984) Stoichiometries of electron transport complexes in spinach chloroplasts. Arch Biochem Biophys **231:** 378–389

Xiao J, Li J, Ouyang M, Yun T, He B, Ji D, Ma J, Chi W, Lu C, Zhang L (2012) DAC is involved in the accumulation of the cytochrome b_6f complex in Arabidopsis. Plant Physiol **160:** 1911–1922

Yamori W, Evans JR, Von Caemmerer S (2010) Effects of growth and measurement light intensities on temperature dependence of CO_2 assimilation rate in tobacco leaves. Plant Cell Environ **33:** 332–343

Yamori W, Takahashi S, Makino A, Price GD, Badger MR, von Caemmerer S (2011) The roles of ATP synthase and the cytochrome b_6f complexes in limiting chloroplast electron transport and determining photosynthetic capacity. Plant Physiol **155:** 956–962